

Gas migration signatures over the volcanic Cratered Seamount, off the Nicobar Islands in the Andaman Sea

G. Sriram¹, P. Dewangan^{1*}, V. Yatheesh¹, A. Peketi¹, P. Mahesh¹, A. Mazumdar¹, V. P. Mahale¹, J. Jacob¹, K.M. Dubey¹, P. Kumar¹, C.K. Mishra¹, S. Gautham¹, A.K. Anirudh¹, P. Ankush¹, A.B. Madhav Ram¹, K.K. Shijin¹, T.G. Salkar¹, A.S. Zatale^{1,2}, V. Rajurkar^{1,2}, S.H. Khokher¹, S. Garg¹, A.K. Choudhary¹, K. K. Aswini¹, A. Gawas¹

¹CSIR-National Institute of Oceanography, Dona Paula, Goa 403004, India

²Academy of Scientific and Innovative Research (AcSIR), CSIR-National Institute of Oceanography, Dona Paula, Goa 403004, India

*Corresponding author. E-mail: pdewangan@nio.org

Abstract

The submarine volcanic arc off Nicobar is seismologically very active with numerous earthquake swarms reported after the tsunamigenic 26th December 2004 earthquake in the Andaman-Nicobar-Sumatra subduction zone. Therefore, we carried out multiple high-resolution multibeam echo-sounding (MBES) surveys along with water column imaging (WCI) onboard *RV Sindhu Sadhana* along the volcanic arc to detect water column anomalies related to volcanism. We observed for the first-time two gas flares originating from the outer flanks of *Cratered Seamount* (CSM) in the WCI data during the 2018 expedition. The flare on the SE flank of CSM originated at a depth of 710 m and rises to a depth of ~225 m from the ocean surface; whereas the flare on the NW flank of CSM originates at 400 m and rises to ~150-100 m from the ocean surface. We repeated the experiment in November 2021 and remapped the flare on the NW flank of CSM. Further, a new gas flare was observed in a southward direction at an offset of 215 m. This flare which originated at 380 m and rises to 150 m from the ocean surface, was imaged during multiple passes along different radial directions at different times. Geological sampling over the gas venting location shows a large rock sample with a couple of live *Bathymodiolus spp.*, a chemosynthetic species typically observed at methane seeps and/or hydrothermal vent sites. These observations confirm the volcanic activity at the Cratered Seamount located off the Nicobar region in the Andaman Sea.

1. Introduction

Oblique subduction of the Indo-Australian Plate beneath the Southeast Asian Plate leads to the formation of the Trench-Forearc-Volcanic arc-Backarc system in the Andaman-Nicobar-Sumatra region. The volcanic arc consists of a series of volcanoes starting from the sub-aerially exposed Barren and Narcondam volcanoes near the Andaman Islands (Kamesh Raju et al., 2012) to the submarine volcanoes in the off-Nicobar region (Aswini, et al., 2020a; Kamesh Raju et al., 2012; Tripathi et al., 2018). This volcanic arc further extends southward to include the volcanoes in the Sumatra region. Barren is an active volcano (Bandopadhyay et al., 2017; Sheth et al., 2010) whereas Narcondam is believed to be a dormant volcano (Bandopadhyay et al., 2017; Curray, 2005). The Barren Island which was built of prehistoric lava flows with volcanoclastic sediments and became subaerial about 1.6 Ma with major eruptions around 71, 62, 23, 17, and 8 Ka (Ray et al., 2013). Following a period of approximately 200 years of dormancy, the Barren volcano experienced a significant eruption in March 1991. Subsequent eruptions were recorded during the periods of 1994-1995, 2005-2006, 2008-2010 (Sheth et al., 2010) in 2017, 2018-2019 (Gunda et al., 2021), and most recently 2nd May 2023 (Global Volcanism Program, 2023). These eruptions demonstrate the reactivation of volcanic activity within the Barren volcano after a prolonged period of quiescence.

Kamesh Raju et al., (2012) observed a series of submarine volcanoes that connects the Barren Island Volcano to the active volcanoes in the Sumatra region like Marapi and Singgalang. One of the seamounts known as Cratered Seamount (CSM) is located off the Nicobar Islands, and is believed to be active in the recent past. After the destructive megathrust earthquake on 26th December 2004, multiple earthquake swarms were observed near the CSM in the years 2005, 2014, 2015, and 2019 (Kamesh Raju et al., 2012; Kundu et al., 2012; Lay et al., 2005; Aswini et al., 2021; Aswini et al., 2020) and are believed to be associated with the volcano-tectonic activities.

Gas emission signatures associated with submarine volcanoes and hydrothermal vents have been reported worldwide like gas flares at Rota-1 volcanic seamount in the Mariana arc trench (Chadwick et al., 2018, 2014) and Champagne, Eifuku (Lupton et al., 2006), Kolumbo, Greece (Carey et al., 2013), Kick-`em-Jenny crater, Lesser Antilles (Allen et al., 2018), Mid-Okinawa Trough (Nakamura et al., 2015), a hydrothermal system in Guaymas, Southern Trough (Ondréas et al., 2018), etc. The Andaman volcanic arc exhibits geochemical and tectonic similarities to other volcanic arcs such as the Mariana arc (Edward T Baker et al., 2008; Pearce et al., 2005a), Okinawa trough (Shinjo and Kato, 2000a), and Lesser Antilles (Series, 1977). As a result, it is anticipated that gas emissions would occur during its active phase. Therefore, CSIR-NIO carried out multiple high-resolution multibeam echo-sounding (MBES) surveys along with water column imaging (WCI) in

the off-Nicobar region to identify water column anomalies associated with volcanism or magma movement. In the present study, we report for the first-time persistent gas flares over the CSM, located off the Nicobar region in the Andaman Sea.

2. Tectonic setting and geological features

The study area is in the Andaman-Nicobar-Sumatra subduction zone, a seismically active region due to the oblique subduction of the Indo-Australian plate beneath the Southeast Asian plate (Fig.1, (Curry, 2005; Yatheesh et al., 2021)). The northward motion of the Indo-Australian plate is divided into trench-perpendicular motion responsible for subduction and trench-parallel motion, which is largely accommodated by a sliver fault system (Fitch, 1972). The sliver fault comprises of Sagaing Fault (SGF) and Andaman Transform Fault (ATF) in the north, Andaman Backarc Spreading Centre (ABSC) in the middle with segments (A, B, C, D), and Andaman Nicobar Fault (ANF), West Andaman Fault (WAF), the Great Sumatra Fault (GSF) in the south (Curry, 2005; Kamesh Raju et al., 2004; Singh et al., 2013; Yatheesh et al., 2021). As the GSF enters the Andaman Sea, it splits into two strands: the Aceh Fault (ACF) and the Seulimeum Fault (SLF). Several other faults exist in the Andaman-Nicobar region like the Eastern Margin Fault (EMF), which is defined by the edge of the Andaman-Nicobar Islands, and N-S trending Diligent Fault (DLF). Towards the east of DLF lies a shallower N-S-aligned ridge known as the Invisible Bank (IB) (Moeremans and Singh, 2015; Singh et al., 2013; Yatheesh et al., 2021). Several geomorphologic features exist in the Andaman-Nicobar region such as trench, forearc, volcanic arc, and the back-arc basin (Curry, 2005; Kamesh Raju et al., 2004; Roy and Das Sharma, 1993). A prominent depth depression on the depth chart defines the trench to the south as 10°N ; however, the trench's signature is attenuated northward by 10°N as it is overlaid by sediments from the Bengal and Nicobar fans. The forearc region comprises accretionary prism sediments, a forearc high, and a forearc basin. The basin is bounded by the Invisible Bank (IB) in the east and EMF in the west and is covered with 3-5 km thick sediments of Cenozoic age north of the Nicobar Islands. The volcanic arc system consists of an active Barren Volcano (Bandopadhyay et al., 2017; Sheth et al., 2010), a dormant Narcondum volcano (Bandopadhyay et al., 2017; Curry et al., 1979; K. a. Kamesh Raju et al., 2012), 32 submarine volcanoes ranging from $6^{\circ}26'\text{N}$ to $10^{\circ}58'\text{N}$ (Aswini et al., 2020; Kamesh Raju et al., 2020, 2012; Tripathi et al., 2018), and aerial volcanism in the southern Java and Sumatra regions. The Andaman Backarc Basin (ABB) evolved because of the breakup and dispersal of the conjoint Alcock-Sewell Seamount complex (Curry et al., 1979; Kamesh Raju et al., 2012; Yatheesh et al., 2021).

During the India NGHP Expedition-01, deep drilling and coring activities in the forearc region specifically at Site NGHP-01-17 discovered gas hydrate deposits within ash beds and ash-rich

zones starting approximately 250 m beneath the seafloor and extending towards the bottom-simulating reflector (BSR). The expedition also yielded a long sedimentary record of approximately 700 m. This sedimentary record has proven to be highly valuable in understanding the volcanic history of the region, covering a span from the Cenozoic era to the present as evidenced by distinct volcanic ash beds (Cawthern et al., 2010; Badesab et al., 2021; Rodolfo, 1969). These ash layers have been linked to volcanic activity in the Andaman region since the Miocene epoch (Cawthern et al., 2010; Collett et al., 2008).

3. Data acquisition and processing

3.1. Bathymetry Data

High-resolution Multibeam bathymetry (MBES) and water column image (WCI) data were acquired onboard *RV Sindhu Sadhana* using hull-mounted hydroacoustic equipment (Hydrosweep DS-3, ATLAS hydrographic, GmbH, Bremen, Germany) during the SSD-046 cruise (March 2018) and a repeat survey is carried out during the SSD-085 cruise (November 2021) in the off Nicobar region (Fig. 1). The center frequency was set to be 15.5 kHz, with 256 beams and the data were acquired for full-ocean depth. The bathymetry data were processed by applying the sound velocity profile data acquired during the cruise and removing various noise, outliers, and any other sonar artifacts by manual editing using Teledyne PDS software v4.3. Finally, a grid was generated with a spatial resolution of a 50m grid for the interpretation of the seafloor features. The bathymetry corresponding to the Cratered Seamount is shown in Figure 2a. Similar to the present multibeam bathymetry survey was conducted in 2011 over the twin seamounts to study the morphology of the earthquake swarm region (K. A. Kamesh Raju et al., 2012). The multibeam data was collected with the SIMRAD EM120 multibeam echosounder system typically operates at 12kHz with a total number of 111 beams. Along with the multibeam bathymetry data and TV-guided grab samples are collected and no significant signatures of gas plumbing are observed within the TV-guided grab video footage. The timelapse multibeam bathymetry data acquired in 2018 and 2021 is acquired using Hydrosweep DS-3 multibeam echosounder system typically operates at 15.5 kHz with a total of 256beams and capable of visualizing the objects or features within the water column itself, such as gas plumes, fish schools, or other marine organisms. It provides a comprehensive understanding of the entire water column, from the seafloor to the surface, enabling researchers to gather valuable data about the marine environment and its inhabitants.

3.2. Water column imaging and processing

The water column image (WCI) data recorded by the MBES is used primarily to detect the acoustic scatters due to fish, gas bubbles, and other biomass in the water column. The gas flares appear as sub-vertical continuous structures in the water column as compared to other undesired signals (Veloso et al., 2015). To improve the signal-to-noise ratio, we stacked four to five WCI using an indigenously developed MATLAB code (Fig. 3 and 4). We attempt to identify the root of gas flares by accounting for the multi-beam swath, minimum slant range, and side lobes due to the first reflection of the acoustic signal from the seafloor (Hughes Clarke, 2006; Urban et al., 2017). In the present study, the gas flares are detected within the minimum slant range and close to the center lobe. Multiple transits (Fig. 2a, NW-SE and EW (white dashed) in 2018 and NE-SW and EW (green dashed) in 2021) over Cratered Seamount are also analyzed to characterize the temporal variation in the intensity of observed gas flares (Fig. 3 and 4).

3.3. Subbottom Profiling

The shallow subsurface sedimentary and water column imaging is obtained using the hull-mounted ATLAS Teledyne Parasound P35 sub-bottom profiler (SBP) system, which provides a depth range of 10 m to 11000 m and sediment penetration of 150 m with parametric mode dual-frequency of 18 kHz – 24 kHz (Primary High Frequency; PHF). The non-linear interference of primary signals generates secondary parametric high (37– 42 kHz; SHF) and parametric low (0.5 – 4 kHz; SLF) frequencies. The SLF records provide a subsurface penetration maximum of up to 150 m while the SHF records provide high-resolution gas bubble signatures in the water column. The PHF and SLF data were processed using Seismic UNIX software with a band-pass filter (200 – 6000 Hz) for removing high and low-frequency noise. The PHF data show multiple gas flares, which rise to a height of 150-200 m from the surrounding seafloor depth of 380 m (Fig. 4d).

4. Results

4.1. The volcanic seamount S13 (Cratered Seamount)

Cratered Seamount (SM13 of Tripathi et al., 2018) is located at 7° 56.2533'N and 94° 02.3704'E in the off-Nicobar region. The seamount has an approximate diameter of 7 km and rises to 1500 m (SM13) above the surrounding seafloor depth of 2000 m (Fig. 2a). The summit of SM13 is 160 m deep and shows a couple of prominent breaches in the NW direction. The SW flank region shows several volcanic cones within the valley of the seamount. The seamount displays a steep slope ranging from 12° to 40° over the flanks in NW and SW directions and across a slumped feature

in the SE direction of the seamount (Fig. 2b). In contrast, most of the region within the crater shows gentle slopes ($< 5^\circ$) barring some ridges.

4.2. Fluid/gas migration from the Cratered Seamount

We imaged the first-time gas flares over the submarine Cratered Seamount in 2018 as well as 2021. Figures 3 and 4 show stacks of WCI with date, time, and location for observed gas flares in 2018 and 2021, respectively. In 2018, we observed two gas flares on the SE and NW flanks of the CSM. A giant plume-like feature (GF1, Fig. 3a) was identified on the SE flank of the crater at 03:08:08 AM (GMT) on 2 March 2018 (Location: 7.9299°N, 94.0499°E) during the NW transit (marked as Tr-1 in Fig. 2). The plume started at ~715 m water depth and spreads horizontally after rising ~225 m above the seafloor (Fig. 3a). The gas flare (GF2, Fig. 3b) located towards the NW of the crater is identified at 11:40:21 AM (GMT) (02/03/2018, 7.94°N/94.0399°E) during the NW transit. The gas flare, observed at 400 m water depth, rises to ~300 m above the seafloor. The GF2 (Fig. 3c) was imaged again during the west-to-east transit (marked as Tr-2 in Fig. 2a) at 12:56:45 PM (GMT) (02/03/2018, 7.94°N/94.0399°E) and no significant variation is observed within an hour.

The MBES and WCI survey was repeated in 2021 to re-image the observed gas flares over the crater seamount to understand its temporal variation (Fig. 4). Gas flare (GF2) is imaged at 07:59:02 AM (GMT) (20/11/2021, 7.94°N/94.0399°E) (Fig. 4a). A new gas flare (GF3) is imaged at 215 m southward of GF2 on the NW flank of CSM at 01:33:37 PM (GMT) (20/11/2021, 7.9380°N/94.04°E) (Fig. 4b). The gas flare GF3, observed at 380 m, rises to ~150 m above the seafloor. The stack image of GF3 from transit lines oriented in NNE-SSW and EW directions shows that the gas flare (GF3) is almost vertical near the seafloor and shows a minor deflection after a rise of 150 m. The high-frequency SBP data (PHF; Fig. 4d) also imaged the gas flare at a water depth of 380 m, which rises to 200 m in the Dynamic Positioning (DP) of the ship. Likewise, the MBES backscatter images also identified the gas flare (Fig. 4e) as a high amplitude feature within the nadir range. The Geological sampling over the gas venting location over the crater seamount shows a large volcanic rock sample with a couple of live *Bathymodiolus spp.* (Fig.5a-d) a chemosynthetic species typically observed at methane seeps sites (Mazumdar et al., 2019) and at hydrothermal vents (Lin et al., 2021).

5. Discussion

5.1. Active fluid/gas migration above the Cratered Seamount

A high-resolution multibeam survey provides detailed geomorphology of the crater seamount (SM13) and associated signatures of fluid/gas migration in WCI as a plumed-shaped gas flare that

rises vertically up to a certain depth and then spread horizontally and vertical gas flares that rise from the seafloor to shallower depths. In the absence of the geological and geochemical information derived from the samples collected from this gas flare region, we attempt to provide a reasonable explanation for the formation of these gas flares based on generalized information derived from a similar situation in different parts of the globe. In cold seep systems, hydrate-coated methane bubbles constitute the gas flares (Dewangan et al., 2020; Gros et al., 2019; Martínez-Carreño and García-Gil, 2013; Tréhu, 2003) while liquid droplets of CO₂ coated with CO₂-hydrate constitute the gas flares in a hydrothermal vent (Chadwick et al., 2014) and thermal vents (Nakamura et al., 2015). In general, the methane-related gas flares rise to the gas hydrate stability zone (GHSZ) which is around ~700 m in the Indian continental margins (Dewangan et al., 2020), whereas CO₂ hydrate-coated bubble may rise to ~500 m water depth (Nakamura et al., 2015) and even shallower water depths of ~150 m (Chadwick et al., 2014). At depths shallower than the hydrate stability zone, the coating disappears and the gases dissolve rapidly in the seawater. In the present study, the flare starts at depths of 500 m within the CO₂ gas hydrate stability zone and rises to a depth of ~144 m (Figs. 3 and 4). Due to the vertical rise of these flares, we presume that the flares are formed due to gases rather than hydrothermal fluids. Further, the shallow depths of flares suggest the presence of CO₂. Similar gas flares due to CO₂ droplets are reported worldwide such as Rota-1 (Chadwick et al., 2018, 2014) and Champagne, Eifuku (Lupton et al., 2006) in the Mariana arc, Mid-Okinawa Trough (Nakamura et al., 2015), a hydrothermal system in Guaymas, Southern Trough (Ondréas et al., 2018), submarine volcano Kolumbo, Greece (Carey et al., 2013), Kick-`em-Jenny crater, Lesser Antilles (Allen et al., 2018), etc. The Andaman volcanic arc is geochemically and tectonically analogous to the Mariana arc (Edward T. Baker et al., 2008; Pearce et al., 2005b), Okinawa trough (Shinjo and Kato, 2000b), and Lesser Antilles (Series, 1977), and therefore, we presume that the flare's composition is predominantly CO₂. However, further geological/geochemical study is warranted to confirm the composition of gas flares in Andaman's volcanic arc system.

In contrast to buoyant gases, hydrothermal plumes rise at high temperatures and are warmer than the surrounding seawater. Later, the plume cools and stays at a particular depth in equilibrium in the density stratification of the water column (Gartman and Findlay, 2020). We identified a plume-like signature over the Cratered Seamount (SM13) that rises to a height of ~144 m from the crater summit (Fig. 3a) and spread horizontally. The geological, geochemical, and petrographic studies of SM13 showed that the seamount was hydrothermally active in the recent past (K. A. Kamesh Raju et al., 2012; L. et al., 2020; Saha et al., 2020) like other volcanic arcs such as the Kurile arc (Glasby et

al., 2006), the Lesser Antilles arc in the Caribbean Sea (Calais et al., 2002) and the Mariana arc (Edward T. Baker et al., 2008).

5.2. Frequent earthquake swarms near the volcanic arc

The mega-thrust tsunamigenic earthquake (M_w 9.1) in December 2004 resulted in an earthquake swarm in 2005 January in the volcanic arc region off Nicobar with more than 150 events with $M_w \geq 5$ and > 600 teleseismically recorded events (Lay et al., 2005). This region also witnesses other earthquake swarms in 2014, 2015, and 2019 and got widespread attention as many researchers focused on understanding the origin of these swarms (Aswini et al., 2020). Kamesh Raju et al., (2012) mapped the volcanic arc region and showed a well-developed Cratered Seamount. The geological and geochemical studies analysis showed that the seamount was active in the recent past (Surya Prakash et al., 2012). Kundu et al (2012) showed that the swarm occurs due to strike-slip and normal faults, indicating a volcano-tectonic origin and fluid flow plays an important role in triggering the aftershock events or swarms. Global Centroid-Moment-Tensor (CMT) of 2005 earthquake swarms indicate magmatic dyke intrusions along the weak zones (Mukhopadhyay & Dasgupta, 2008). Frequent earthquake swarms are typically attributed to a critical stage of the magma chamber beneath the volcanoes; therefore, even small stress changes may trigger earthquake swarms (Špičák et al., 2009; Špičák and Vaněk, 2016, 2013). The passive Ocean Bottom Seismometer (OBS) experiment reported a high magnitude earthquake (M_w 6.5) on 21st March followed by a swarm (Dewangan et al., 2018). Very long-period events (VLPEs) along with the hydroacoustic phase are observed near the volcanic arc indicating the unrest of the subsurface magma chamber. The bimodal distribution of the b-value from the 2014 earthquake swarms also suggests the dominance of both tectonic and volcanic activities (Aswini et al., 2021). Frequent earthquake swarms in the volcanic arc from 2005 to 2019 may indicate magmatic dyke intrusions like that reported in central Japan (Ukawa and Tsukahara, 1996). Thus, the volcanic arc in the Andaman Sea is dominated by tectonic processes driven by shallow magma movement. Therefore, we propose that the gas flares over the Cratered Seamount may be associated with gases released from the subsurface magma chamber through dyke intrusions.

6. Conclusions

We report for the first-time gas flares in the volcanic arc region of the Andaman Sea near the Cratered Seamount (CSM). The initial observation of these gas flares occurred in 2018 in close proximity to the CSM. A subsequent multibeam echo-sounding (MBES) survey conducted in 2021 confirmed the presence of gas flares over the CSM. In general, the gas flares terminate at shallower

depths of ~150 m, which may represent the boundary of the CO₂ hydrate stability zone; therefore, we propose that the gas composition may be dominated by CO₂ as reported in other worldwide submarine volcanoes. The geological sample collection over the CSM shows the presence of live *Bathymodiolus* spp. a chemosynthetic species typically observed at methane seeps sites and at hydrothermal vents suggesting gas venting at the CSM location. The region has experienced frequent earthquake swarms, indicating unrest in the shallow subsurface magma chamber. Therefore, we propose that gases are likely being released from the subsurface magma chamber through dyke intrusions.

Acknowledgments

The authors are grateful to Prof. Sunil Kumar Singh, Director of CSIR-NIO, for permission to publish this paper. We are grateful to the Captain and Crew of *RV Sindhu Sadhana* and the CSIR-NIO Research Vessel Management team (Mr. Kallathian M., Mr. Buddhadas Patole, and Mr. Kuldeep Kumar) for their excellent technical support during the SSD-046 and SSD-085 expeditions aboard *RV Sindhu Sadhana*. The work is done under the CSIR MLP2017 (TeaM-RiSe) program and the NIO contribution no. is XXXX.

Funding:

The authors would like to thank the Council of Scientific and Industrial Research (CSIR) for providing financial support under the CSIR MLP2017 (TeaM-RiSe) program.

Conflicts of interest/Competing interests: The authors declare that they have no competing interests

Data and materials availability:

All data needed to evaluate the conclusions in the paper are present in the paper and the authors don't have any rights to share the data

Code availability:

Commercial Software Teledyne is used to process the Data

Author contribution

Sriram Gullapalli: Conceptualization, Methodology, Visualization, Validation, and Writing - original draft, data curation, P. Dewangan: original draft improvement, Visualization, V. Yatheesh: Original draft, Visualization, A. Peketi: original draft improvement, Visualization, A. Mazumdar: original draft improvement, Visualization. K.M. Dubey: original draft improvement, Visualization,

P. Kumar: original draft improvement, Visualization, C.K. Mishra, P. Mahesh, V. P. Mahale, S. Gautham, A.K. Anirudh, Ankush, A.B. Madhav Ram, K.K. Shijin, T.G. Salkar, A.S. Zatale, V. Rajurkar, S.H. Khokher, S. Garg, A.K. Choudhary: 2021 Expedition data acquisition Team. J. Jacob, K. K. Aswini, A. Gawas: 2018 Expedition data acquisition Team

Ethics approval:

This material is the authors' own original work, which has not been previously published elsewhere. The paper is not currently being considered for publication elsewhere. The paper reflects the author's own research and analysis in a truthful and complete manner.

Consent to participate: Not applicable

Consent for publication: Not applicable

References

- Allen, R.W., Berry, C., Henstock, T.J., Collier, J.S., Dondin, F.J.Y., Rietbrock, A., Latchman, J.L., Robertson, R.E.A., 2018. 30 Years in the Life of an Active Submarine Volcano: A Time-Lapse Bathymetry Study of the Kick-'em-Jenny Volcano, Lesser Antilles. *Geochemistry, Geophysics, Geosystems* 19, 715–731. <https://doi.org/10.1002/2017GC007270>
- Aswini, K. K., Dewangan, P., Kamesh Raju, K.A., Yatheesh, V., Singha, P., Arya, L., Ramakrushana Reddy, T., 2020. Sub-surface magma movement inferred from low-frequency seismic events in the off-Nicobar region, Andaman Sea. *Sci Rep* 10. <https://doi.org/10.1038/s41598-020-78216-2>
- Aswini, K K, Dewangan, P., Raju, K.A.K., Yatheesh, V., Singha, P., 2020. Sub - surface magma movement inferred from low - frequency seismic events in the off - Nicobar region , Andaman Sea. *Sci Rep* 1–13. <https://doi.org/10.1038/s41598-020-78216-2>
- Aswini, K.K., Kamesh Raju, K.A., Dewangan, P., Yatheesh, V., Singha, P., Ramakrushana Reddy, T., 2021. Seismotectonic evaluation of off Nicobar earthquake swarms, Andaman Sea. *J Asian Earth Sci* 221, 104948. <https://doi.org/https://doi.org/10.1016/j.jseaes.2021.104948>
- Baker, Edward T, Embley, R.W., Walker, S.L., Resing, J. a., Lupton, J.E., Nakamura, K.I., de Ronde, C.E.J., Massoth, G.J., 2008. Hydrothermal activity and volcano distribution along the Mariana arc. *Journal of Geophysical Research: Solid Earth* 113, 1–16. <https://doi.org/10.1029/2007JB005423>
- Baker, Edward T., Embley, R.W., Walker, S.L., Resing, J.A., Lupton, J.E., Nakamura, K.I., de Ronde, C.E.J., Massoth, G.J., 2008. Hydrothermal activity and volcano distribution along the Mariana arc. *J Geophys Res Solid Earth* 113, 1–16. <https://doi.org/10.1029/2007JB005423>

- Bandopadhyay, P.C., Carter, a, 2017. Chapter 2 Introduction to the geography and geomorphology of the Andaman–Nicobar Islands. Geological Society, London, Memoirs 47, 9–18. <https://doi.org/10.1144/M47.2>
- Bandopadhyay, P.C., Ghosh, B., Carter, A., 2017. Chapter 16 Natural resources. Geological Society, London, Memoirs 47, 225–232. <https://doi.org/10.1144/M47.16>
- Calais, E., Mann, P., Glen, M., Pamela, J., 2002. Strain partitioning and fault slip rates in the northeastern Caribbean from GPS measurements 29, 2–5. <https://doi.org/10.1029/2002GL015397>
- Carey, S., Nomikou, P., Bell, K.C., Lilley, M., Lupton, J., Roman, C., Stathopoulou, E., Bejelou, K., Ballard, R., 2013. Co2 degassing from hydrothermal vents at kolumbo submarine volcano, greece, and the accumulation of acidic crater water. *Geology* 41, 1035–1038. <https://doi.org/10.1130/G34286.1>
- Cawthern, T., Johnson, J., Bryce, J., Blichert-Toft, J., Flores, J., 2010. A ~9.4 Ma Ash Record from the Andaman Accretionary Wedge: Petrochemical Implications for Arc Evolution, in: AGU Fall Meeting Abstracts.
- Chadwick, W.W., Merle, S.G., Baker, E.T., Walker, S.L., Resing, J. a., Butterfield, D. a., Anderson, M.O., Baumberger, T., Bobbitt, A.M., 2018. A recent volcanic eruption discovered on the central mariana back-arc spreading center. *Front Earth Sci (Lausanne)* 6, 1–16. <https://doi.org/10.3389/feart.2018.00172>
- Chadwick, W.W., Merle, S.G., Buck, N.J., Lavelle, J.W., Resing, J. a., Ferrini, V., 2014. Imaging of CO2 bubble plumes above an erupting submarine volcano, NW Rota-1, Mariana Arc. *Geochemistry, Geophysics, Geosystems* 15, 4325–4342. <https://doi.org/10.1002/2014GC005543>
- Collett, T.S., Haa, Q.C., Cochran, J.R., Boswell, R., Sathe, A. V, 2008. Indian continental margin gas hydrate prospects: Results of the Indian national gas hydrate program (NGHP) expedition 01.
- Curry, J.R., 2005. Tectonics and history of the Andaman Sea region. *J Asian Earth Sci* 25, 187–232. <https://doi.org/10.1016/j.jseaes.2004.09.001>
- Curry, J.R., Moore, D.G., Lawver, L.A., Emmel, F.J., Raitt, R.W., Henry, M., Kieckhefer, R., 1979. Tectonics of the Andaman Sea and Burma, in: *Geological and Geophysical Investigations of Continental Margins*. American Association of Petroleum Geologists. <https://doi.org/10.1306/M29405C12>
- Dewangan, P., Reddy, R., Kamesh Raju, K.A., Singha, P., Aswini, K.K., Yatheesh, V., Samudrala, K., Shuhail, M., 2018. Nature of the ambient noise, site response, and orientation of ocean-bottom seismometers (OBSs): Scientific results of a passive seismic experiment in the andaman sea. *Bulletin of the Seismological Society of America* 108, 248–259. <https://doi.org/10.1785/0120170163>

- Dewangan, P., Sriram, G., Kumar, A., Mazumdar, A., Peketi, A., Mahale, V., Reddy, S.S.C., Babu, A., 2020. Widespread occurrence of methane seeps in deep-water regions of Krishna-Godavari basin, Bay of Bengal. *Mar Pet Geol* 104783. <https://doi.org/10.1016/j.marpetgeo.2020.104783>
- Fitch, T.J., 1972. Plate convergence, transcurrent faults, and internal deformation adjacent to Southeast Asia and the Western Pacific. *J Geophys Res Solid Earth* 77, 4432–4460. <https://doi.org/10.1029/JB077i023p04432>
- Gartman, A., Findlay, A.J., 2020. Impacts of hydrothermal plume processes on oceanic metal cycles and transport. *Nat Geosci* 13, 396–402. <https://doi.org/10.1038/s41561-020-0579-0>
- Glasby, G.P., Cherkashov, G.A., Gavrilenko, G.M., 2006. Submarine hydrothermal activity and mineralization on the Kurile and western Aleutian island arcs, N . W . Pacific 231, 163–180. <https://doi.org/10.1016/j.margeo.2006.06.003>
- Global Volcanism Program, 2023. Report on Barren Island (India).
- Gros, J., Schmidt, M., Dale, A.W., Linke, P., Vielstädte, L., Bigalke, N., Haeckel, M., Wallmann, K., Sommer, S., 2019. Simulating and Quantifying Multiple Natural Subsea CO₂ Seeps at Panarea Island (Aeolian Islands, Italy) as a Proxy for Potential Leakage from Subseabed Carbon Storage Sites. *Environ Sci Technol* 53, 10258–10268. <https://doi.org/10.1021/acs.est.9b02131>
- Gunda, G.K.T., Champatiray, P.K., Chauhan, M., Chauhan, P., Ansary, M., Singh, A., Ketholia, Y., Balaji, S., 2021. Modelling of volcanic ash with HYSPLIT and satellite observations: a case study of the 2018 Barren Island volcano eruption event, Andaman Territory, India. *Curr Sci* 121, 529–538. <https://doi.org/10.18520/cs/v121/i4/529-538>
- Hughes Clarke, J.E., 2006. Applications of multibeam water column imaging for hydrographic survey. *Hydrographic Journal* 3–14.
- Kamesh Raju, K. a., Ray, D., Mudholkar, A., Murty, G.P.S., Gahalaut, V.K., Samudrala, K., Paropkari, a. L., Ramachandran, R., Surya Prakash, L., 2012. Tectonic and volcanic implications of a cratered seamount off Nicobar Island, Andaman Sea. *J Asian Earth Sci* 56, 42–53. <https://doi.org/10.1016/j.jseaes.2012.04.018>
- Kamesh Raju, K.A., Aswini, K.K., Yatheesh, V., 2020. Tectonics of the Andaman Backarc Basin—Present Understanding and Some Outstanding Questions BT - The Andaman Islands and Adjoining Offshore: Geology, Tectonics and Palaeoclimate, in: Ray, J.S., Radhakrishna, M. (Eds.), . Springer International Publishing, Cham, pp. 237–259. https://doi.org/10.1007/978-3-030-39843-9_12
- Kamesh Raju, K.A., Ramprasad, T., Rao, P.S., Ramalingeswara Rao, B., Varghese, J., 2004. New insights into the tectonic evolution of the Andaman basin, northeast Indian Ocean. *Earth Planet Sci Lett* 221, 145–162. [https://doi.org/10.1016/S0012-821X\(04\)00075-5](https://doi.org/10.1016/S0012-821X(04)00075-5)
- Kamesh Raju, K. A., Ray, D., Mudholkar, A., Murty, G.P.S., Gahalaut, V.K., Samudrala, K., Paropkari, A.L., Ramachandran, R., Surya Prakash, L., 2012. Tectonic and volcanic implications of a cratered seamount off Nicobar Island, Andaman Sea. *J Asian Earth Sci* 56, 42–53. <https://doi.org/10.1016/j.jseaes.2012.04.018>

- Kamesh Raju, K A, Ray, D., Mudholkar, A., Murty, G.P.S., Gahalaut, V.K., Samudrala, K., Paropkari, A.L., Ramachandran, R., Surya Prakash, L., 2012. Tectonic and volcanic implications of a cratered seamount off Nicobar Island, Andaman Sea. *J Asian Earth Sci* 56, 42–53. <https://doi.org/10.1016/j.jseaes.2012.04.018>
- L., S.P., Ray, D., B., N.N., Satyanarayanan, M., Kamesh, K.R., Kurian, J.P., M., D.K., a., S.R., 2020. Anomalous phase association of REE in ferromanganese crusts from Indian mid-oceanic ridges: Evidence for large scale dispersion of hydrothermal iron. *Chem Geol* 549, 119679. <https://doi.org/10.1016/j.chemgeo.2020.119679>
- Lay, T., Kanamori, H., Ammon, C.J., Nettles, M., Ward, S.N., Aster, R.C., Beck, S.L., Bilek, S.L., Brudzinski, M.R., Butler, R., Others, 2005. The great Sumatra-Andaman earthquake of 26 december 2004. *Science* (1979) 308, 1127–1133.
- Lin, G., Lu, J., Sun, Z., Xie, J., Huang, J., Su, M., Wu, N., 2021. Characterization of tissue-associated bacterial community of two *Bathymodiolus* species from the adjacent cold seep and hydrothermal vent environments. *Science of the Total Environment* 796, 149046. <https://doi.org/10.1016/j.scitotenv.2021.149046>
- Lupton, J., Butterfield, D., Lilley, M., Evans, L., Nakamura, K.I., Chadwick, W., Resing, J., Embley, R., Olson, E., Proskurowski, G., Baker, E., De Ronde, C., Roe, K., Greene, R., Lebon, G., Young, C., 2006. Submarine venting of liquid carbon dioxide on a Mariana Arc volcano. *Geochemistry, Geophysics, Geosystems* 7. <https://doi.org/10.1029/2005GC001152>
- Martínez-Carreño, N., García-Gil, S., 2013. The Holocene gas system of the Ría de Vigo (NW Spain): Factors controlling the location of gas accumulations, seeps and pockmarks. *Mar Geol* 344, 1–19. <https://doi.org/10.1016/j.margeo.2013.07.012>
- Mazumdar, A., Dewangan, P., Peketi, A., Gullapalli, S., Kalpana, M.S., Naik, G.P., Shetty, D., Pujari, S., Pillutla, S.P.K., Gaikwad, V. V., 2019. The first record of active methane (cold) seep ecosystem associated with shallow methane hydrate from the Indian EEZ. *Journal of Earth System Science* 128, 1–8.
- Moeremans, R.E., Singh, S.C., 2015. Fore-arc basin deformation in the Andaman-Nicobar segment of the Sumatra-Andaman subduction zone: Insight from high-resolution seismic reflection data. *Tectonics* 34, 1736–1750. <https://doi.org/10.1002/2015TC003901>
- Nakamura, K., Kawagucci, S., Kitada, K., Kumagai, H., Takai, K., Okino, K., 2015. Water column imaging with multibeam echo-sounding in the mid-Okinawa Trough: Implications for distribution of deep-sea hydrothermal vent sites and the cause of acoustic water column anomaly. *Geochem J* 49, 579–596. <https://doi.org/10.2343/geochemj.2.0387>
- Ondréas, H., Scalabrin, C., Fouquet, Y., Godfroy, A., 2018. Recent high-resolution mapping of Guaymas hydrothermal fields (Southern Trough). *BSGF - Earth Sciences Bulletin* 189. <https://doi.org/10.1051/bsgf/2018005>
- Pearce, J. a., Stern, R.J., Bloomer, S.H., Fryer, P., 2005a. Geochemical mapping of the Mariana arc-basin system: Implications for the nature and distribution of subduction components. *Geochemistry, Geophysics, Geosystems* 6. <https://doi.org/10.1029/2004GC000895>

- Pearce, J. a., Stern, R.J., Bloomer, S.H., Fryer, P., 2005b. Geochemical mapping of the Mariana arc-basin system: Implications for the nature and distribution of subduction components. *Geochemistry, Geophysics, Geosystems* 6. <https://doi.org/10.1029/2004GC000895>
- Ray, J.S., Pande, K., Awasthi, N., 2013. A minimum age for the active Barren Island volcano, Andaman Sea. *Curr. Sci* 104, 934–939.
- Rodolfo, K.S., 1969. Bathymetry and marine geology of the andaman basin, and tectonic implications for southeast asia. *Bulletin of the Geological Society of America* 80, 1203–1230. [https://doi.org/10.1130/0016-7606\(1969\)80\[1203:BAMGOT\]2.0.CO;2](https://doi.org/10.1130/0016-7606(1969)80[1203:BAMGOT]2.0.CO;2)
- Roy, S.K., Das Sharma, S., 1993. Evolution of Andaman forearc basin and its hydrocarbon potential. *Proceedings of the Second Seminar on Petroliferous Basins of India*. Indian Petroleum Publishers, Dehra Dun, India 1, 407–434.
- Saha, A., Mudholkar, A. V, Kamesh Raju, K. a., 2020. Magma genesis at Andaman volcanic arc regime, Northeastern Indian Ocean: Role of slab-mantle interaction. *Episodes* 43, 323–334. <https://doi.org/10.18814/epiiugs/2020/020019>
- Series, A., 1977. *Geochemistry of the Lesser Antilles volcanic island arc* 41.
- Sheth, H.C., Ray, J.S., Bhutani, R., Kumar, A., Awasthi, N., 2010. The latest (2008--09) eruption of Barren Island volcano, and some thoughts on its hazards, logistics and geotourism aspects. *Curr Sci* 620–626.
- Shinjo, R., Kato, Y., 2000a. Geochemical constraints on the origin of bimodal magmatism at the Okinawa Trough, an incipient back-arc basin. *Lithos* 54, 117–137. [https://doi.org/10.1016/S0024-4937\(00\)00034-7](https://doi.org/10.1016/S0024-4937(00)00034-7)
- Shinjo, R., Kato, Y., 2000b. Geochemical constraints on the origin of bimodal magmatism at the Okinawa Trough, an incipient back-arc basin. *Lithos* 54, 117–137. [https://doi.org/10.1016/S0024-4937\(00\)00034-7](https://doi.org/10.1016/S0024-4937(00)00034-7)
- Singh, S.C., Moeremans, R., McArdle, J., Johansen, K., 2013. Seismic images of the sliver strike-slip fault and back thrust in the Andaman-Nicobar region. *J Geophys Res Solid Earth* 118, 5208–5224. <https://doi.org/10.1002/jgrb.50378>
- Špičák, A., Vaněk, J., 2016. Earthquake swarms reveal submarine magma unrest induced by distant mega-earthquakes: Andaman Sea region. *J Asian Earth Sci* 116, 155–163. <https://doi.org/10.1016/j.jseas.2015.11.017>
- Špičák, A., Vaněk, J., 2013. Earthquake clustering in the tectonic pattern and volcanism of the Andaman Sea region. *Tectonophysics* 608, 728–736. <https://doi.org/10.1016/j.tecto.2013.08.007>
- Špičák, A., Vaněk, J., Hanuš, V., 2009. Seismically active column and volcanic plumbing system beneath the island arc of the Izu-Bonin subduction zone. *Geophys J Int* 179, 1301–1312. <https://doi.org/10.1111/j.1365-246X.2009.04375.x>

- Surya Prakash, L., Ray, D., Paropkari, A.L., Mudholkar, A. V., Satyanarayanan, M., Sreenivas, B., Chandrasekharam, D., Kota, D., Kamesh Raju, K.A., Kaisary, S., Balaram, V., Gurav, T., 2012. Distribution of REEs and yttrium among major geochemical phases of marine Fe–Mn-oxides: Comparative study between hydrogenous and hydrothermal deposits. *Chem Geol* 312–313, 127–137. <https://doi.org/10.1016/j.chemgeo.2012.03.024>
- Tréhu, A.M., 2003. Seismic and seafloor evidence for free gas, gas hydrates, and fluid seeps on the transform margin offshore Cape Mendocino. *J Geophys Res* 108, 2263. <https://doi.org/10.1029/2001JB001679>
- Tripathi, S.K., Varghese, S., Raghav, S., 2018. Morphology of submarine volcanic seamounts from inner volcanic arc of Andaman Sea.
- Ukawa, M., Tsukahara, H., 1996. Earthquake swarms and dike intrusions off the east coast of Izu Peninsula, central Japan. *Tectonophysics* 253, 285–303. [https://doi.org/10.1016/0040-1951\(95\)00077-1](https://doi.org/10.1016/0040-1951(95)00077-1)
- Urban, P., Köser, K., Greinert, J., 2017. Processing of multibeam water column image data for automated bubble/seep detection and repeated mapping. *Limnol Oceanogr Methods* 15, 1–21. <https://doi.org/10.1002/lom3.10138>
- Veloso, M., Greinert, J., Mienert, J., De Batist, M., 2015. A new methodology for quantifying bubble flow rates in deep water using splitbeam echosounders: Examples from the Arctic offshore NW-Svalbard. *Limnol Oceanogr Methods* 13, 267–287. <https://doi.org/10.1002/lom3.10024>
- Yatheesh, V., Aswini, K.K., Kamesh Raju, K.A., John Savio, J., Gawas, A., Dewangan, P., 2021. Morphotectonic signatures and revised timing of opening of the Andaman Backarc Basin, Northeast Indian Ocean. *Tectonophysics* 820, 229108. <https://doi.org/https://doi.org/10.1016/j.tecto.2021.229108>

Figure Captions

Figure.1. Figure Caption: Generalized tectonic map of the Andaman-Nicobar-Sumatra Subduction Zone and adjacent regions, overlaid on global gridded bathymetry (GEBCO_2020), incorporating regional tectonic features from Yatheesh et al. (2021). Shipborne Multibeam bathymetry data from Kamesh Raju et al. (2012) and additional data from 2018 (SSD-046) and 2021 (SSD-085) were utilized. Solid red triangles indicate subaerial volcanoes including Barren and Narcondam islands (Bandopadhyay, 2017). Yellow-filled red triangles represent submarine volcanoes forming a volcanic arc (Aswini et al., 2020), while the yellow-filled red star denotes the Cratered Seamount.

Figure.2. Multibeam bathymetry and slope map of the Cratered Seamount in the Andaman Sea. a) Multibeam bathymetry map (acquired in 2018) shows transits (2018 (white dashed) and 2021 (green dashed)) and identifies the locations of three gas venting signatures, along with the timing of the Sonar wedge when the features are detected. b) Slope map of the Cratered Seamount highlighting the positions of the gas venting signatures.

Figure.3. Multibeam and water column imaging (WCI) snapshots of the 2018 (SSD-046) expedition over the Cratered Seamount: a) Sonar wedge 2-D stack of Gas flare (GF1) along ship track (Tr1, Fig.2) with time stamp, b) Sonar wedge 2-D stack of Gas flare (GF2) along ship track (Tr1, Fig.2) with time stamp, and c) Sonar wedge 2-D stack of Gas flare (GF2) along ship track (Tr2, Fig.2) with a time stamp.

Figure.4. Multibeam and water column imaging (WCI) 2-D stack snapshots over the Cratered Seamount from the 2021 (SSD-085) expedition: a) Sonar wedge 2-D stack view of Gas flare (GF2) along ship track (Tr3, Fig.2) with time stamp, b) Sonar wedge 2-D stack view of Gas flare (GF3) along ship track (Tr3, Fig.2) with time stamp, c) 3-D stack view of the Sonar wedge of Gas flare (GF3) after outlier filtering along ship tracks (Tr3 and Tr4, Fig.2), d) Subbottom profiling data highlighting the gas flare (GF3), and e) Backscatter image from MBES highlighting the gas flare marked in the yellow ellipse.

Figure.5. Geological sample collected from the crater seamount within the vicinity of the gas flare. a) Rock sample collected using the grab sampler and live *Bathymodiolus spp.* the chemosynthetic community is attached to the rock sample. b) Rock sample scaled of 30cm×12cm. c) outer shell of live *Bathymodiolus spp.* and d) internal structure of the *Bathymodiolus spp.*

Figure.1.

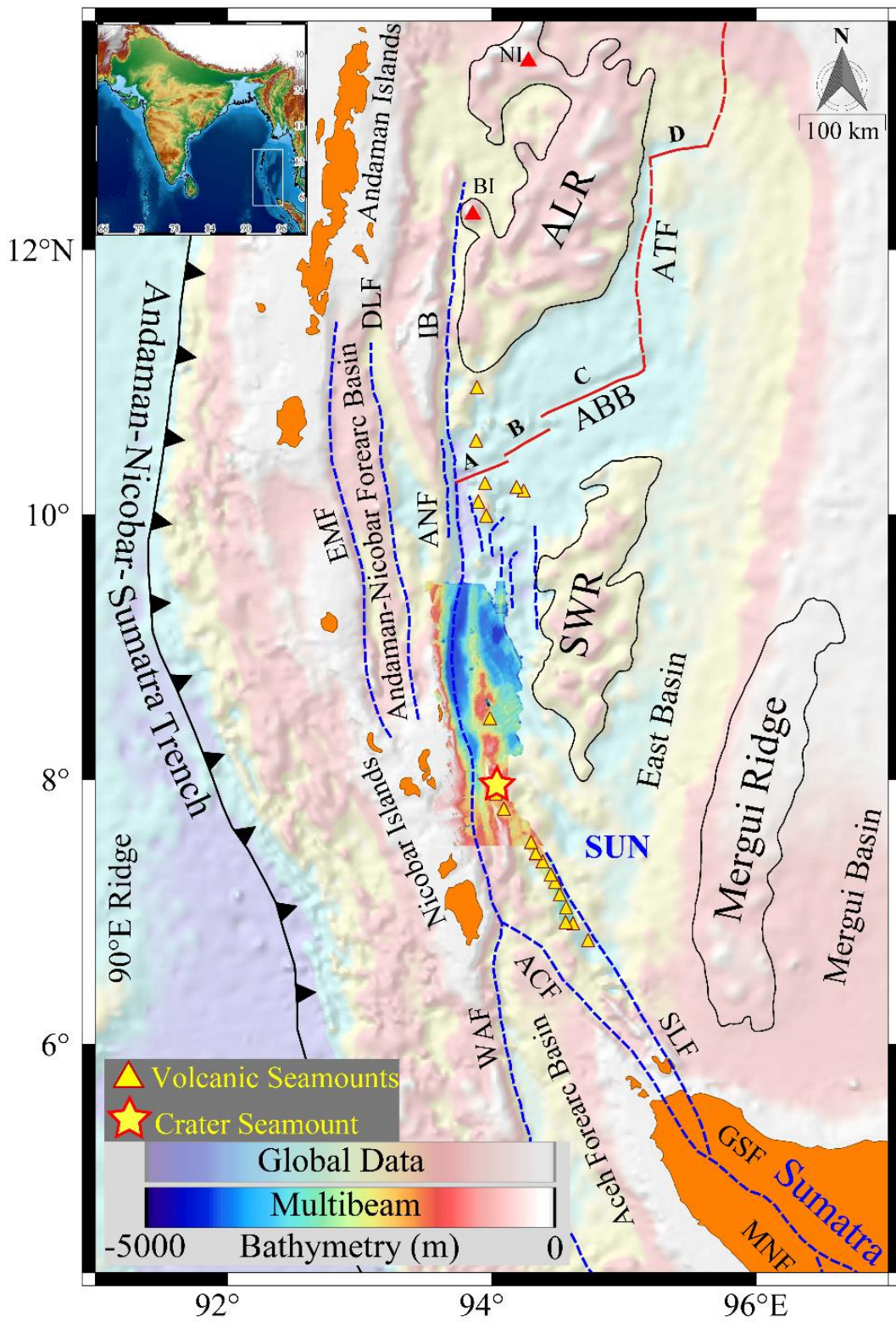


Figure.2.

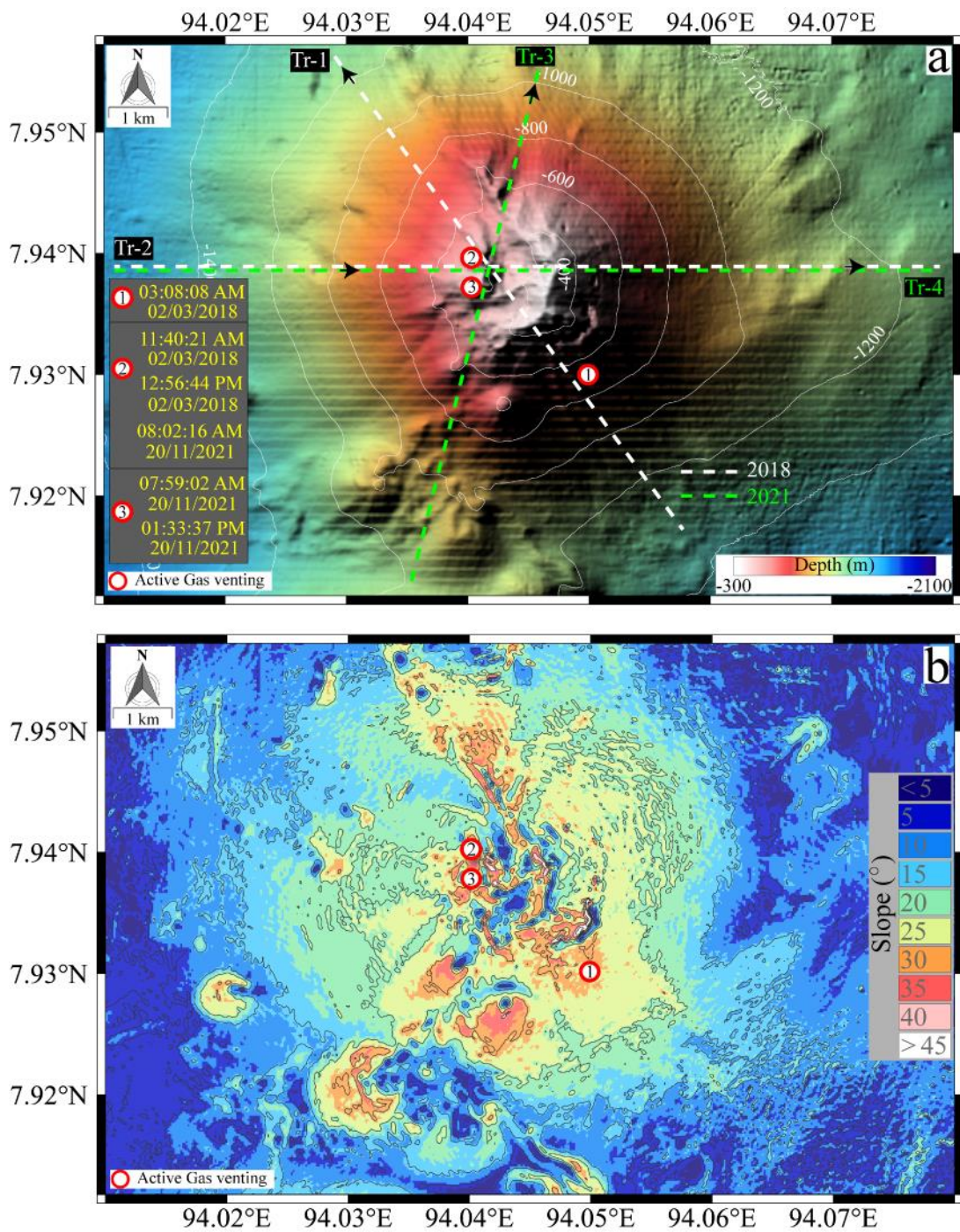


Figure.3.

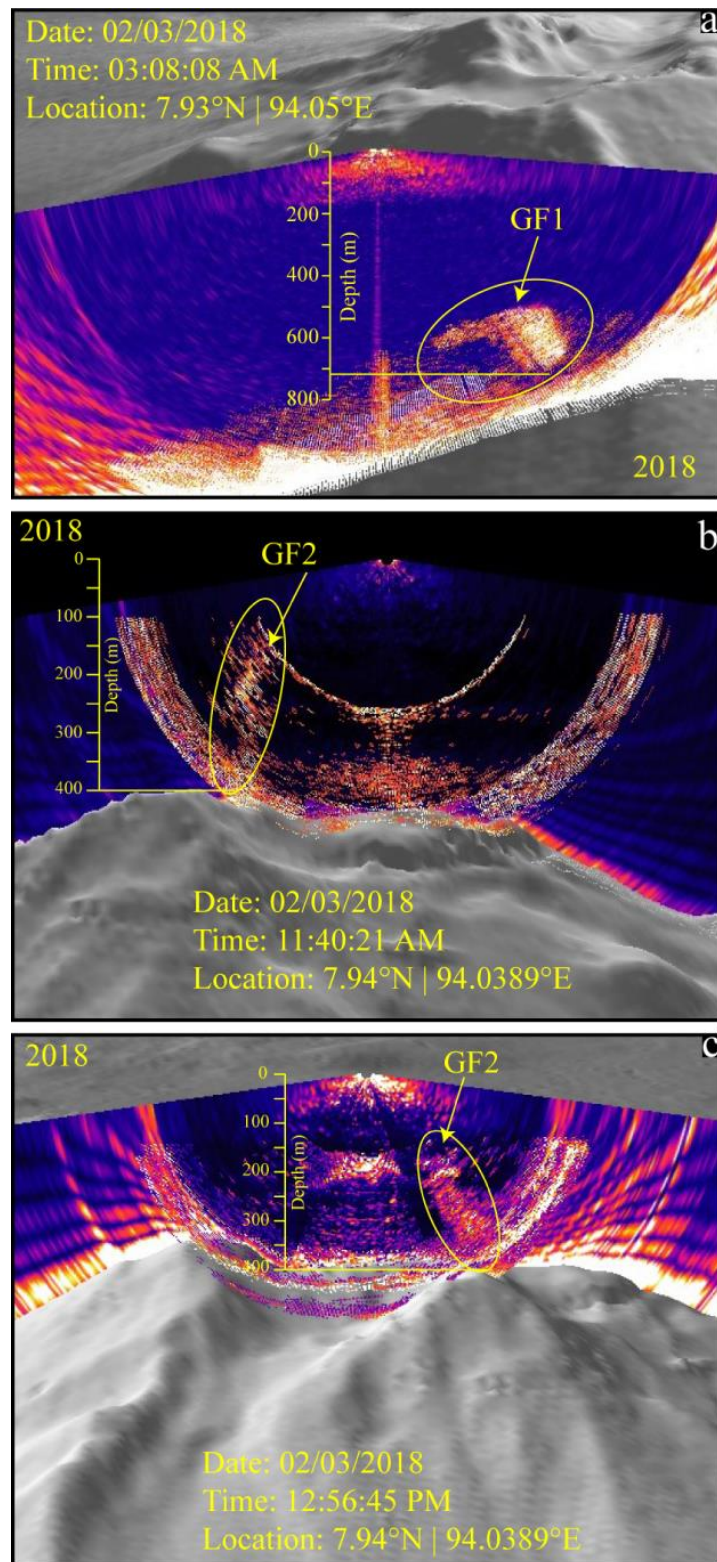


Figure.4.

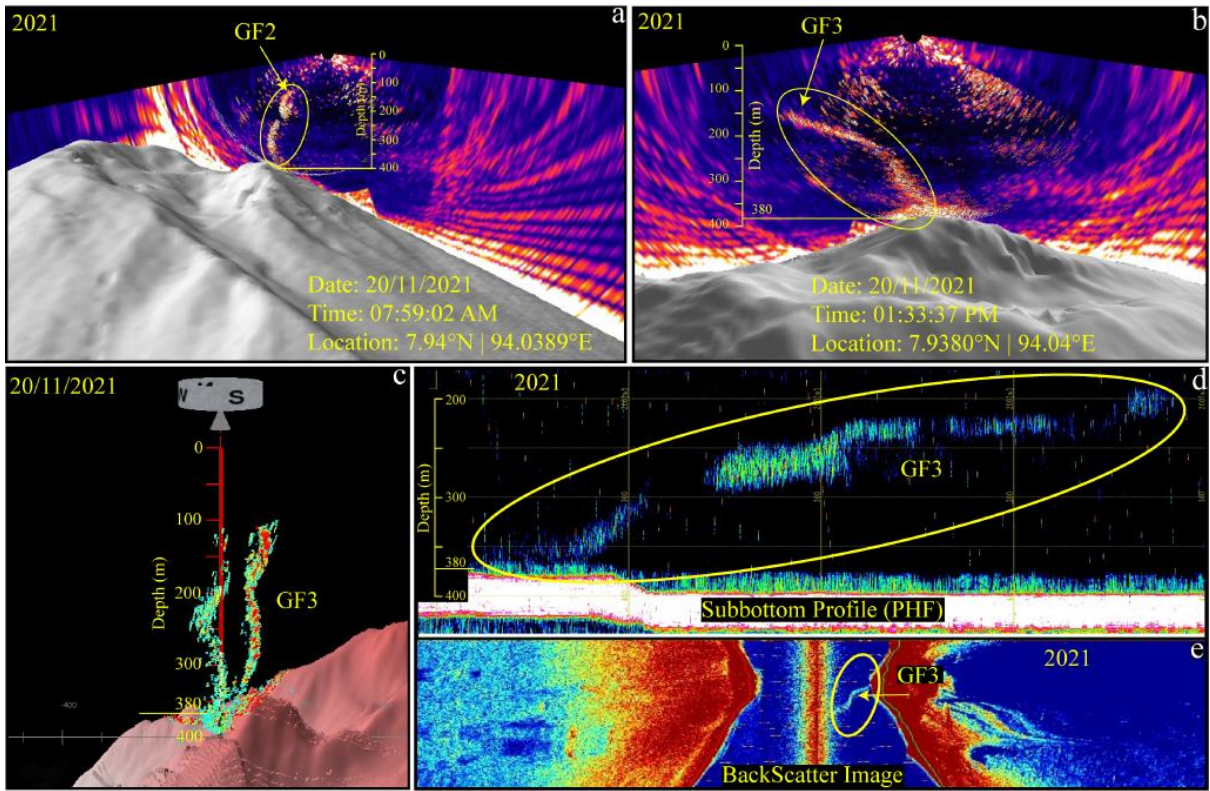


Figure.5.

